SUPPLEMENTARY INFORMATION

Disinfection of constructed wetland effluent by in situ electrochemical chlorine production for water reuse

Suanny Mosquera-Romero[1,2,3], Antonin Prévoteau[1,4], Jan B.A. Arends[1,4], Diederik P.L. Rousseau[3], Luis Dominguez-Granda[2], Korneel Rabaey[1,4]†

[1] *Center for Microbial Ecology & Technology (CMET), Ghent University, Coupure Links 653, B-9000 Gent, Belgium*

[2] *ESPOL Polytechnic University, Escuela Superior Politécnica del Litoral, ESPOL, Centro del Agua y Desarrollo Sustentable, Facultad de Ciencias Naturales y Matemáticas, FCNM, P.O. Box 09-01-5863, Guayaquil, Ecuador*

[3] *Department of Green Chemistry and Technology, Ghent University, Graaf Karel de Goedelaan 5, B-8500 Kortrijk, Belgium*

[4]*Center for Advanced Process Technology for Urban Resource Recovery (CAPTURE), Coupure Links 653, 9000 Ghent, Belgium. www.capture-resources.be*

†*Corresponding author*

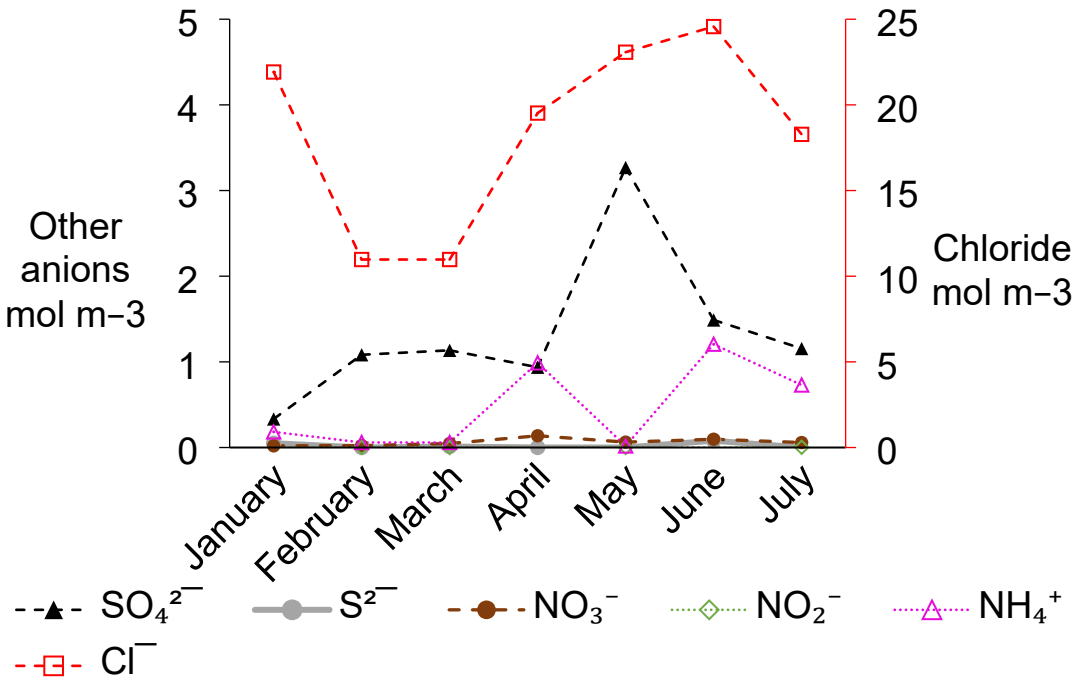

Figure S1. Ionic composition of the Ecuadorian constructed wetland effluent from January until July 2019.

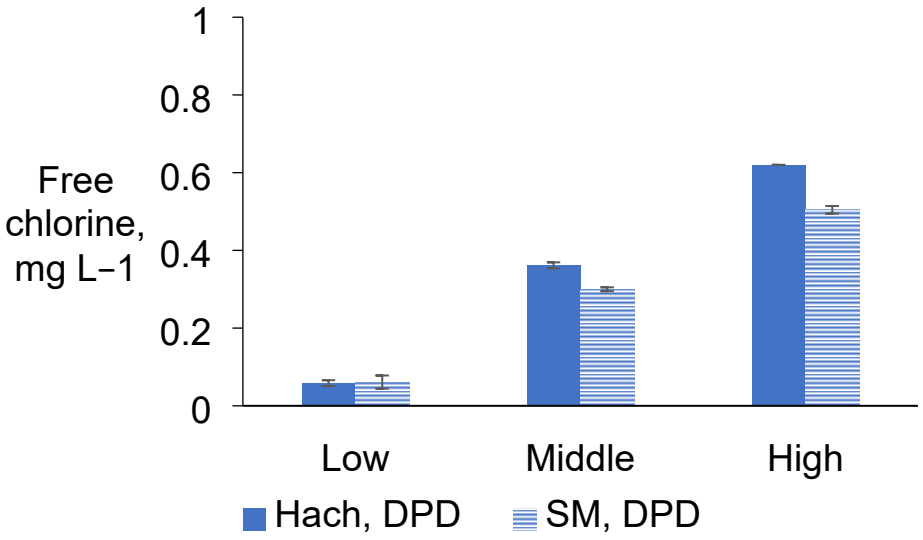

Figure S2. Comparison of the results from the DPD colorimetric methods used in this study by diluted solution from the standard NIST(PourRite, Hach) at 26.9 ± 0.06 mg L^{-1}. The legend HACH represents the results from the method provided by the company in HACH photometers, and SM was the standard method performed in the spectrophotometer Biochrome WPA1100nm. Concentrations are represented as given by the equipment in mg L^{-1}. The maximum difference is 0.1 mg L^{-1} observed at the higher measured standard.

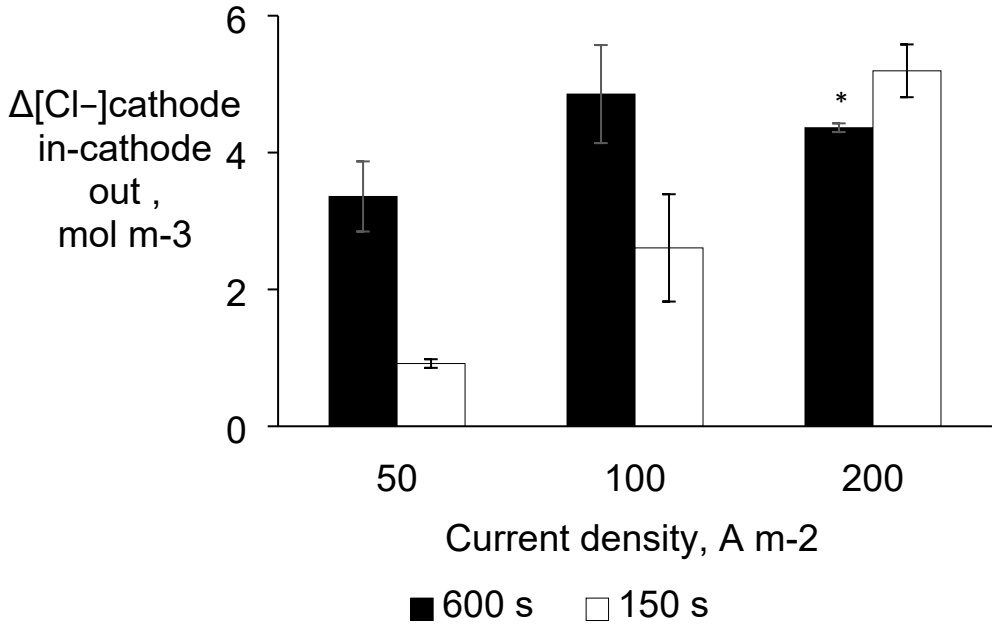

Figure S3. Transported chloride (y-axes) to the anolyte through an anion exchange membrane *vs*. the different current densities tested (x-axes) at the two highest anodic hydraulic retention time: 600s (flow of 0.3×10^{-6} m^3 s^{-1}) and 150s (flow of 1.3×10^{-6} m^3 s^{-1}). The transported chloride was determined as the difference between the chloride concentration before and after passing through the cathodic chamber. *Power supply on the day of this experiment was not providing a fixing current (1.7-2 A in 0.01 m^2 anode), so values could be slightly underestimated

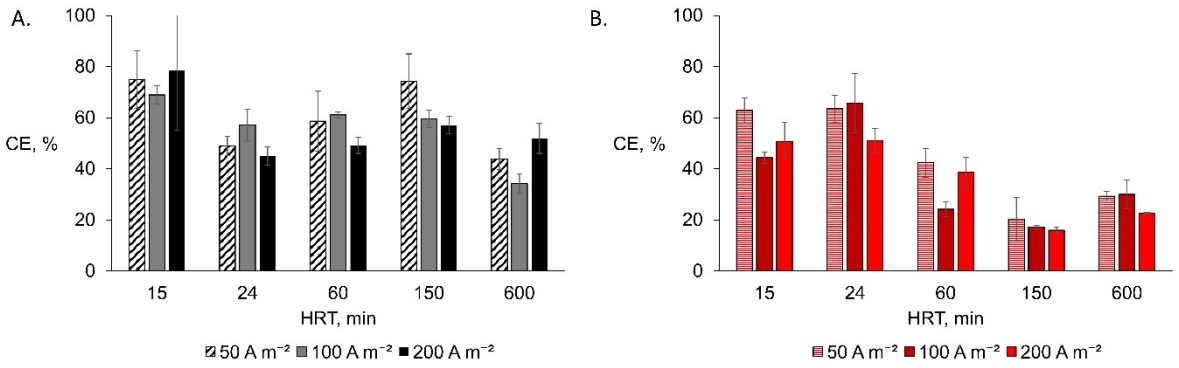

Figure S4. Coulombic efficiency (CE,%) in the function of flow rate when a two-chamber electrochemical cell was divided by **A.** an anion exchange membrane (AEM) or by **B.** a cation exchange membrane (CEM) during the continuous flow of an aqueous solution containing 18.47 mol Cl^- m^{-3}.

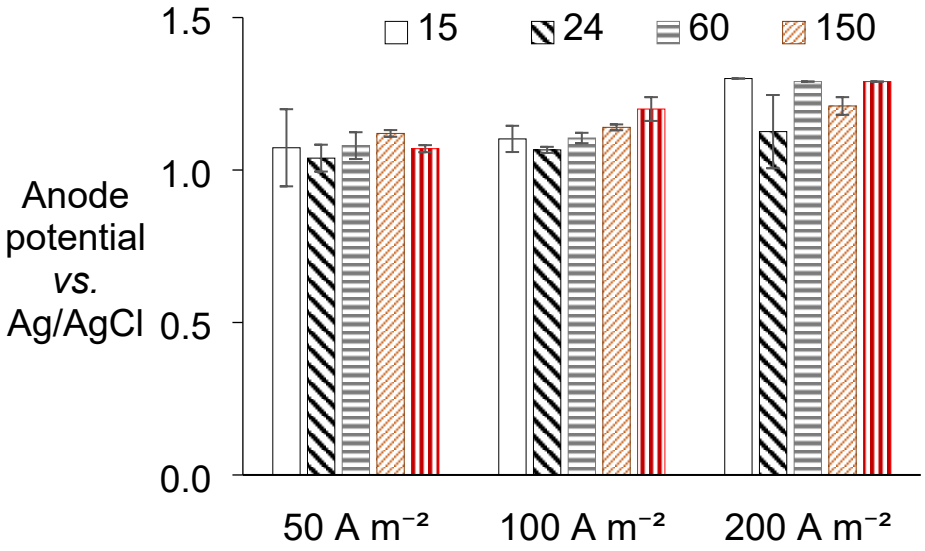

Figure S5. Anode potential in function of the current density applied (50,100,200 A m^{-2}). The legends indicate the HRT(15,24,60,150,600 s) of the anodic chamber during the experiments. Data was collected from the Datalogger (Voltacraft DL190V, Germany) every 5 min during experimentation, error bar represents standard deviation.

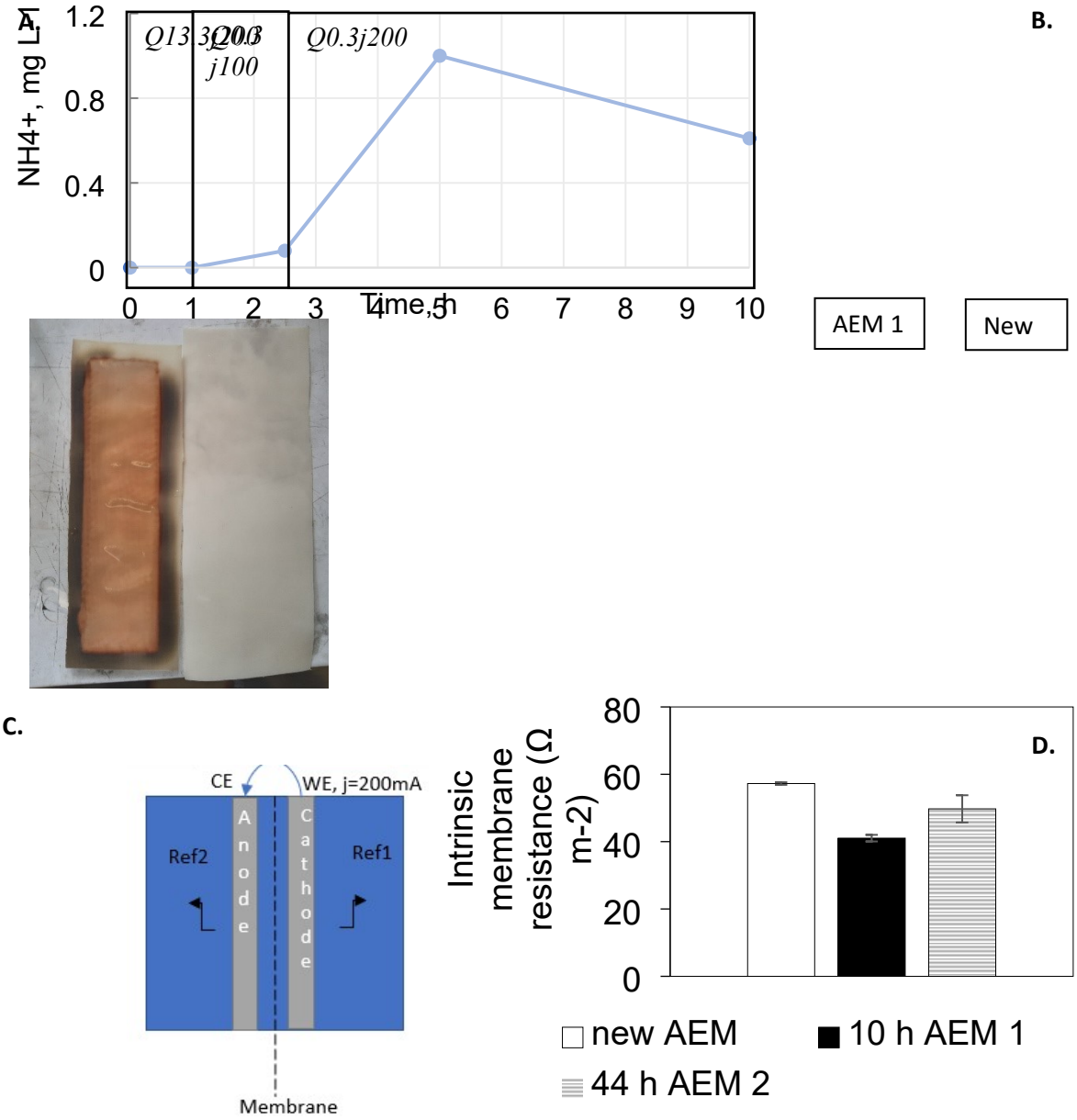

Figure S6. **A**. Ammonium (NH_4^+) release from the AEM membrane detected in the anolyte during electrolysis of NaCl solution at a flow rate of 0.3 × 10^{-6} m^3 s^{-1}. **B.** Photo of a new AEM membrane (right) next to the used one for 10 h during the experiments (AEM1) **C.** Diagram of the current interrupt tests performed with an electrolyte of 1 M NaCl solution in a two-chamber cell, each chamber with an Ag/AgCl reference electrode (Ref1, Ref2) close to the working (WE) and counter (electrode), respectively. **D.** Measured intrinsic membrane resistance of a new AEM (blue), AEM1(brown) after 10 h of operation: 2 h at 0.3 × 10^{-6} m^3 s^{-1} 1 A and 7 h at 0.3 × 10^{-6} m^3 s^{-1} 2 A, and AEM2(orange) after 44 h of operation: 22 h at 0.3 × 10^{-6} m^3 s^{-1} 0.5 A and 22 h at 0.3 × 10^{-6} m^3 s^{-1} 1 A.

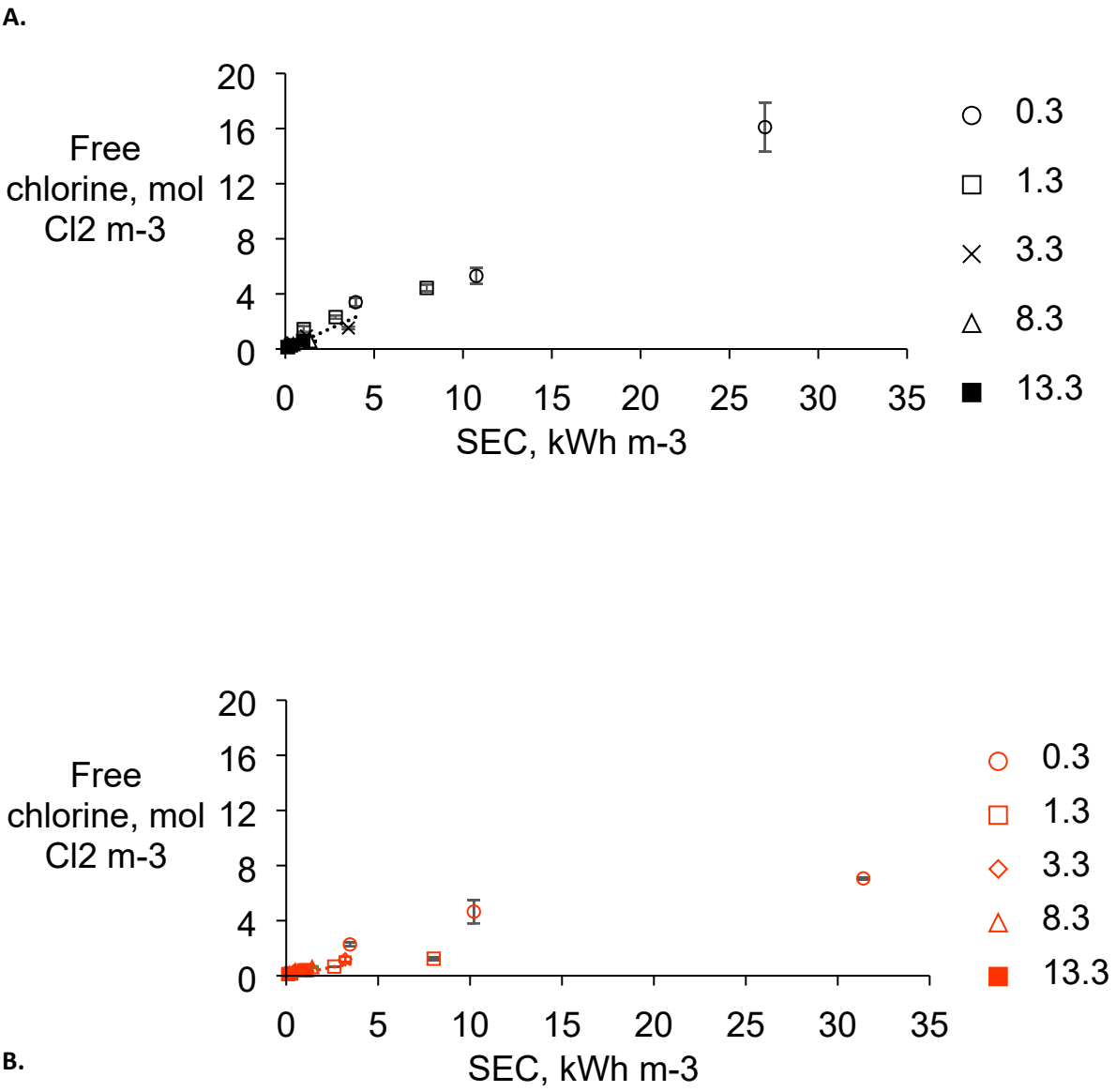

Figure S7. Free chlorine production *vs.* specific energy consumption (SEC) of the electrochemical cell during continuous electrolysis of an aqueous solution with 18.47 mol Cl^- m^{-3}. **A.** represents the results using an AEM, and **B.** represents the results using a CEM. The legend represents the flow rate (0.3, 1.3, 3.3, 8.3, 13.3) × 10^{-6} m^3 s^{-1} through the 0.0002 m^3 anodic chamber, meaning an HRT of 600, 150, 60, 15 s, respectively

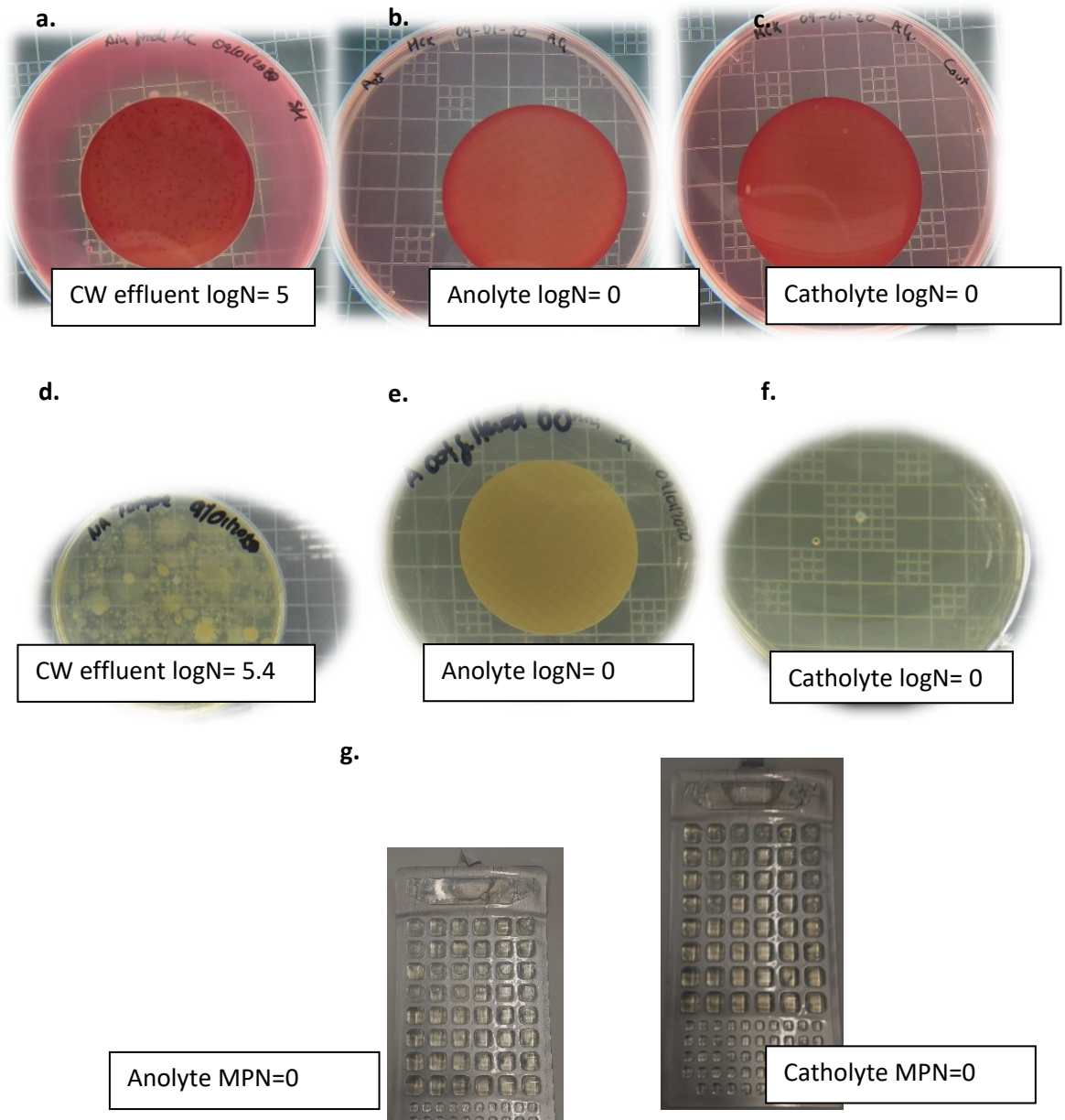

Figure S8. Microbial counting from samples in Ecuador constructed wetland effluent (a. , d). After passing the anodic chamber (b. , e.), and after passing the cathodic chamber (c. , f.) with the MacConkey agar (top) and R2A agar (middle). Collilert-18 results to corroborate microbial plating from the Belgian effluent (g.) after passing the anodic and cathodic compartment.

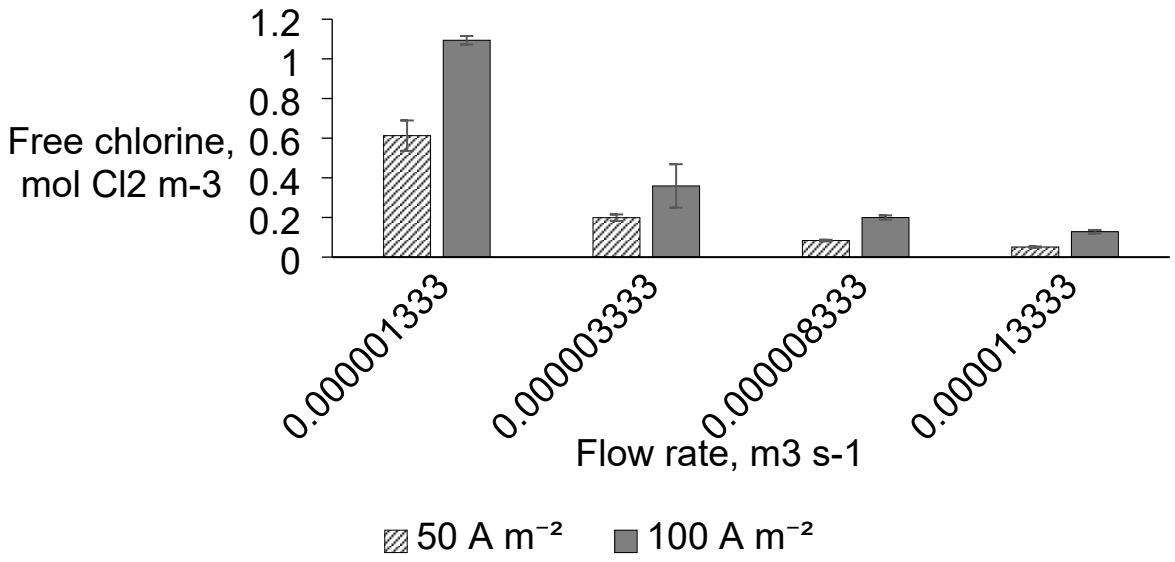

Figure S9. Free chlorine production from low chloride solution of 5.69 mol m^{-3} during continuous flow electrolysis in a two-chamber system separated with an anion exchange membrane. Higher current densities (>100 A m^{-2}) were impossible to achieve as they reached a cell voltage > 30V, which was the limit of the power supply.

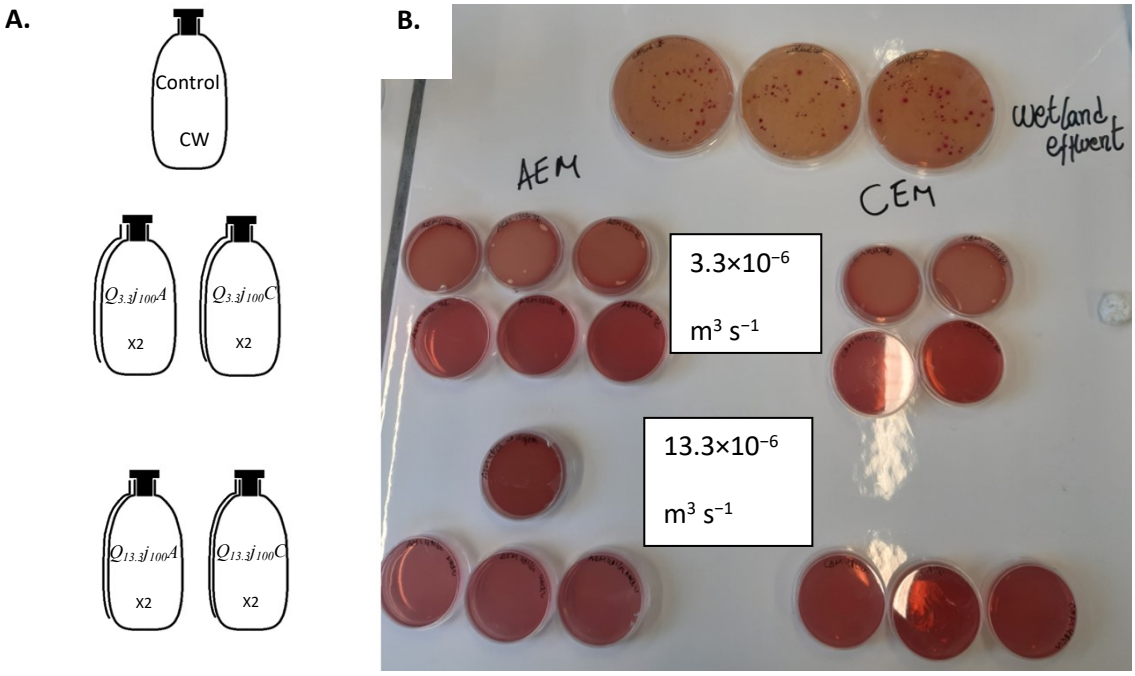

Figure S10. Configuration of the incubation experiment in closed serum bottles of 200 mL(A.). Photo of the MacConkey incubated plates to identify *E.coli* regrowth from the anolyte of the different operational parameters tested at Day 4(B.). At the top: a control of the wetland effluent without disinfection was incubated. At bottom left: results with set-up with anion exchange membrane (AEM)

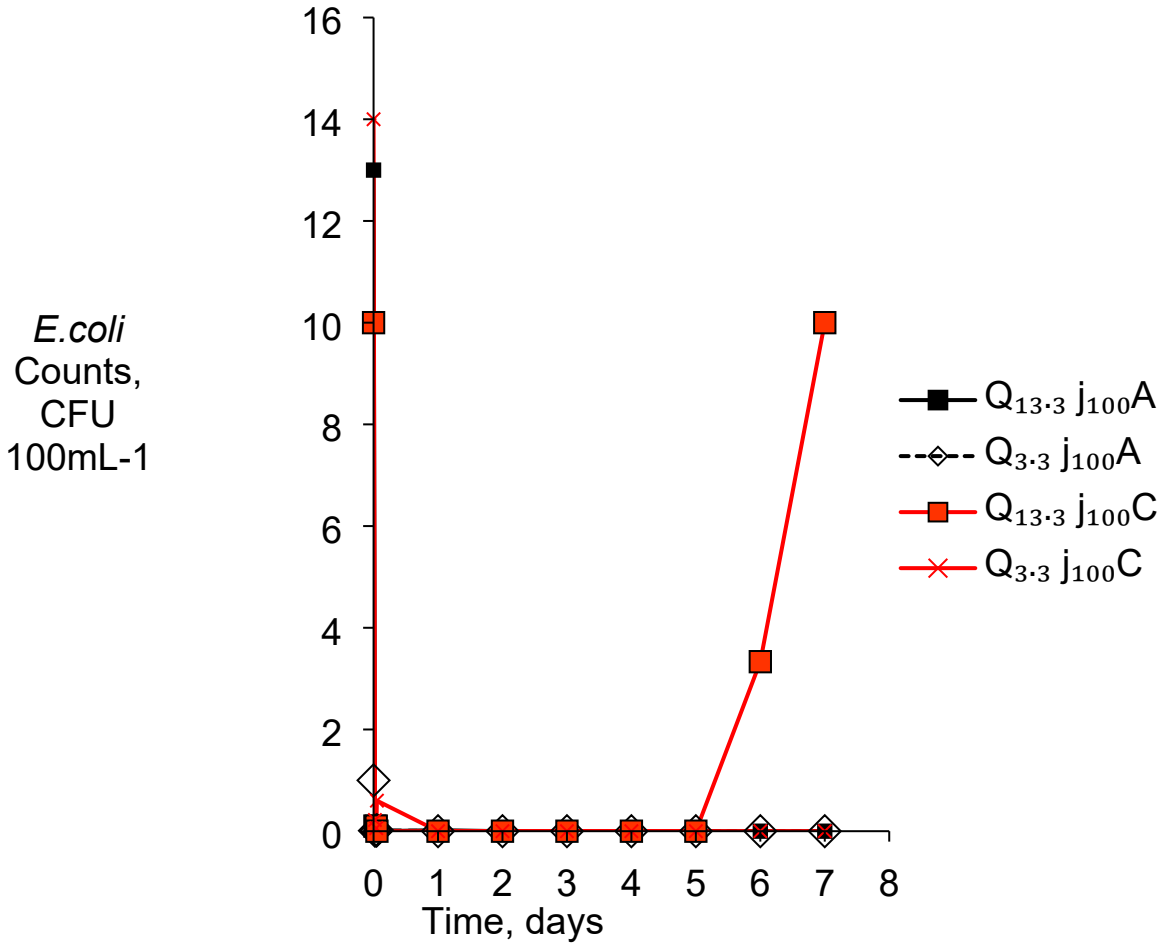

Figure S11. Counting results from the MacConkey agar to identify *E.coli* (red colonies) of an electrolyzed constructed wetland effluent with a chloride content (5.69 ± 2.35 mol Cl^- m^{-3}) in Belgium during 7 days of incubation. The configuration described the settings of flow rate (Q) in $\times 10^{-6}$ m^3 s^{-1} and current density (j) in A m^{-2}; and whether an anion exchange membrane (A) or cation exchange membrane (C) were used.

Table S1. Water quality analysis for constructed wetland (CW) effluents in three monthly (n=3) campaigns used for electro-disinfection in this study. Bellow detection limit (BDL) for NH_4^+ is < 0.01 mg L^{-1}.

Parameter	Units	CW Ecuador	CW Belgium
		Average ± SD (n)	Average ± SD (n)
Temperature	°C	26.7 ± 0.8 (3)	21.7 ± 6.0 (3)
pH	-	6.7 ± 0.1 (3)	7.4 ± 0.2 (3)
Conductivity	mS cm^{-1}	4.0 ± 0.3 (3)	1.7 ± 0.5 (3)
COD	mg L^{-1}	6.5 ± 3.5 (3)	35.2 ± 7.1 (3)
NH_4^+	mg L^{-1}	BDL (3)	61.2 ± 44.1 (3)
Alkalinity	mg $CaCO_3$ L^{-1}	193.0 ± 121.0 (3)	160.4 ± 44.1 (3)
Turbidity	NTU	1.0 ± 0.8 (3)	13.2 ± 1.5 (3)
Hardness	mg $CaCO_3$ L^{-1}	611.0 ± 14.0 (3)	38.2 ± 12.8 (3)
TOC	mg L^{-1}	5.5 ± 3.2 (3)	47.5 ± 10.6 (3)
TSS	mg L^{-1}	13.5 ± 9.6 (2)	12.9 ± 0.7 (2)
VSS	mg L^{-1}	11.1 ± 11.1 (2)	9.7 ± 5.1 (2)
Chloride	mg L^{-1}	745.6 ± 413.3 (3)	223 ± 85.6 (2)
Total counts	CFU $100mL^{-1}$	1.4×10^5 (3)	7.8×10^6 (3)
Fecal counts	CFU $100mL^{-1}$	7.9×10^4 (3)	1.2×10^6 (3)

Table S2. Non-potable water reuse guidelines(g) and mandatory(m) for different countries. CFU= colony-forming units, NTU= Nephelometric Turbidity unit. Redrafted from Leong et al., (2017).

	Fecal coliforms (CFU $100ml^{-1}$)	Total coliforms (CFU $100ml^{-1}$)	Turbidity (NTU)	TSS (mg L^{-1})	DO (min, % sat)	pH (-)
European Commission bathing water (m)	2000	10000	1		80-120	6.0-9.0
China (toilet flushing) (m)		3	5		1	6.0-9.0
California		2.2	2			
France (g)	1000					
Germany(g)	100	500	1-2 (m)	30	80-120	6.0-9.0
Japan (m)	10	10	5			6.0-9.0
Spain(Canary Islands)		2.2	2	3		6.5-8.4
UK bathing water	2000 (m)	10 000 (m)	1		80-120	6.0-9.0
US EPA (g)	14		2			
WHO (irrigation)(m)	1000		10			

Table S3. Reported costs of disinfection units. Data reported in kWh m^{-3} was converted to \$ m^{-3} by considering the cost of 0.3 USD per kWh. Redrafted from (Burch and Thomas, 1998; Gassie and Englehardt, 2017; Norra et al., 2022; Twort et al., 2000).

Disinfection unit	kWh m^{-3}	Capacity cost \$ m^{-3}	Remarks of the calculated energy investment and treatment efficacy
Chlorine / chlorine active	No mentioned	0.77 – 4.19	Production of 0.04 m^3 s^{-1}
Uv radiation + Photovoltaic cells	No mentioned	0.011- 2.7	Small scale (0.01 m^3 s^{-1}) has O&M costs ranging \$2,700 and \$3,300
Ozonation		0.016	10 kWh per kg ozone
Chlorine-free electrochemical disinfection	5.7	1.7	5.5 log removal of *E.Coli*
UV-TiO_2	6.5 /order*	1.95	
UV-H_2O_2	7.0/order*	2.1	*Order of removal of organic contaminant
Peroxone process (O_3+H_2O_2)	2.0/order*	0.6	\$0.55 million annual O&M for a 100 mgd
Ozone-UV	4.0/order*	2.4	

Burch, J.D., Thomas, K.E., 1998. Water disinfection for developing countries and potential for solar thermal pasteurization. Sol. Energy 64, 87–97. https://doi.org/10.1016/S0038-092X(98)00036-X

Gassie, L.W., Englehardt, J.D., 2017. Advanced oxidation and disinfection processes for onsite net-zero greywater reuse: A review. Water Res. 125, 384–399. https://doi.org/10.1016/j.watres.2017.08.062

Leong, J.Y.C., Oh, K.S., Poh, P.E., Chong, M.N., 2017. Prospects of hybrid rainwater-greywater decentralised system for water recycling and reuse: A review. J. Clean. Prod. 142, 3014–3027. https://doi.org/10.1016/j.jclepro.2016.10.167

Norra, G.F., Baptista-Pires, L., Cuervo Lumbaque, E., Borrego, C.M., Radjenovic, J., 2022. Chlorine-free electrochemical disinfection using graphene sponge electrodes. Chem. Eng. J. 430, 132772. https://doi.org/10.1016/j.cej.2021.132772

Twort, A.C., Ratnayaka, D.D., Brandt, M.J.B.T.-W.S. (Fifth E. (Eds.), 2000. Disinfection of water, in: Water Supply. Butterworth-Heinemann, London, pp. 429–XXI. https://doi.org/https://doi.org/10.1016/B978-034072018-9/50011-4